

THE RELIABILITY TEST OF USING THE MODERATE SATELLITE IMAGES FOR METALS CONTAMINATED CORN PLANTS DETECTION IN THE NILE DELTA, EGYPT

Mayie M. AMER¹, Atef M. ELSBAAY²

¹Tanta University, Faculty of Agriculture, Agricultural Engineering Department, Egypt. Phone: 00201202266172, E-mail: mai.amer@agr.tanta.edu.eg

²Kafrelsheikh University, Faculty of Agriculture, Agricultural Engineering Department, Egypt. Phone: 002 01007503876, E-mail: atef.ahmed@agr.kfs.edu.eg

Corresponding author: mai.amer@agr.tanta.edu.eg, mayieamer@yahoo.com

Abstract

For the synoptic assessment of corn plants content of Ca, and K accurate monitoring of land surface dynamics using remote sensing is needed. We looked at a full resolution dataset from the Medium Resolution satellite Imaging (Sentinel-2) as an open source as an alternative to the costly high resolution the more widely used high-resolution satellite Imaging (Worldview2) data for vegetation monitoring. We compared Sentinel-2 image and Worldview 2 data acquired in 2018 with in situ measured hyperspectral data and metal concentrations in plant samples collected from fields in the study area for this purpose. The current research was conducted on the experimental site during the 2018 corn cropping season (Zea Mayz). Results indicated that: The Difference Vegetation Index (DVI), the Enhanced Vegetation Index (EVI), the Green Normalized Difference Vegetation Index (GNDVI), and the Leaf Area Index (LAI) were the more sensitive indicators to Ca and K above ground corn plants content. These VIs had R² values more than 0.5 with the in-situ measurements for the both images. DVI, EVI, and GNDVI performed well in estimating plant dry matter Ca and K content with R² > 0.5, with a high significant level P-value < 0.001 and LAI had a statistically significant impact with a P-value < 0.5 for WV2 image. The Sentinel-2 VIs performed well in estimating plant dry matter Ca and K content with R² values > 0.5, with a high significant level P-value 0.001. LAI had a statistically significant impact with a P-value < 0.5 with Ca concentration and P-value < 0.01 with K concentration. This study suggests that the moderate resolution satellite images can be used for corn plants Ca and K content.

Key words: Change detection, Remote sensing, plant stress, image processing

INTRODUCTION

Plant stress can be tracked in the field using in-field spectroscopy, which is both time and cost efficient [19]. Remote sensing change detection (CD) is commonly defined as a process to identify differences in geographical surface phenomena over time [8, 2]. Techniques of remote sensing (RS) have been shown to be a promising approach for crop development Observing [20], nutrition diagnosis, Identifying the geographical area, detecting and quantifying the types of changes, and finally determining the accuracy effects are all part of the general aim of change detection in remote sensing [11].

This field has attracted a lot of effort in research due to its applications in various areas as Land-use and land-cover (LULC). Vegetation change, Crop monitoring,

Environmental change and crop stress detection [5].

Change detection (CD) on earth's surface is an active research topic since it can help in monitoring and optimal planning of Earth's resources and also help to arrest undesired changes. Any change detection system should be able to (a) define the change area and change rate; (b) distribution of change areas; (c) change trajectories; and (d) the accuracy assessment of the change detection methods [9].

[10, 8] classified CD techniques into (1) comparative analyses based on post-classified data and (2) simultaneous analyses of multitemporal images.

The conventional methods of soil contamination assessment in large areas involve field data collection, chemical analyses in a laboratory as well as

- during a field survey for the cropland test site, and
- from inventory data and visual interpretation of high spatial resolution images for the test site.

Table 1. Sensor's specifications of WorldView 2 and Sentinel 2 Imagery

| Sensor | | |
|------------------------|-------------------|--|
| | WorldView-2 (WV2) | ESA's Sentinel 2 satellite |
| Acquisition date | July 2018 | July 2018 |
| Bands used | 8 | 13 |
| Spectral range (nm) | 450-800 | visible and near-infrared (VNIR) to the short-wave infrared (SWIR) |
| Spatial resolution (m) | 2 | 10 |

Source: WorldView 2 and Sentinel 2 Imagery, July 2018 [18, 12].

A statistical analysis was run on the results. t-test, regression analysis and the significance test were run to find the most sensitive vegetation indices. DVI, EVI, GNDVI, and LAI were the most sensitive VIs to Ca and K concentration accumulated in above ground plant dry matter. Table 2 shows the VIs were determined using ENVI 5.3 software from the WV2 and Sentinel 2 images captured on July 2018.

Table 2. The most sensitive VIs were determined using ENVI 5.3 software from the WV2 and Sentinel 2 images

| Vegetation index | Apriviation | Formula | Reference |
|--|-------------|--|-----------|
| Difference Vegetation Index | DVI | $DVI = NIR - Red$ | [15] |
| Enhanced Vegetation Index | (EVI) | $EVI = 2.5 * \frac{(NIR - Red)}{(NIR + 6 * Red - 7.5 * Blue + 1)}$ | [7] |
| Green Normalized Difference Vegetation Index | (GNDVI) | $GNDVI = \frac{(NIR - Green)}{(NIR + Green)}$ | [6] |
| Leaf Area Index | (LAI) | $LAI = (3.618 * EVI - 0.118)$ | [1] |

Source:
<https://www.13harrisgeospatial.com/docs/vegetationindices.html>, Accessed on July 2018 [17].

RESULTS AND DISCUSSIONS

The WV2 and Sentinel 2 images captured on July 2018 for the summer crop (corn) shown in Fig. (2a and b). The most sensitive VIs

shown in Table 2 correlation coefficients with in situ hyperspectral vegetation indices were computed. The correlation coefficient, regression analysis, and the P-value for this VIs are shown in Table 3.

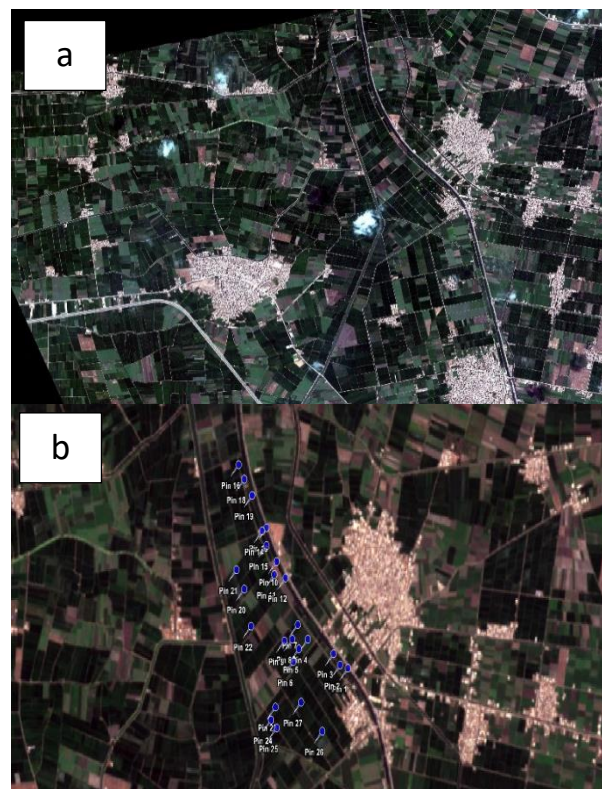


Fig. 2. (a) WorldView2 satellite image and (b) Sentinel 2 satellite image for the study location

Sources:
 (a) European space agency, July2018 [4].
 (b)<https://www.sentinel-hub.com/>, July2018 [13].

Table 3. Validation results of regression coefficient for estimating in-situ hyperspectral vegetation indices depends on hyperspectral vegetation indices calculated from the images

| In-situ VIs | WorldView 2 | | | Sentinel 2 | | |
|-------------|-------------|----------------|----------|------------|----------------|--------------|
| | r | R ² | P-value | r | R ² | P-value |
| DVI | 0.765 | 0.585 | 0.000*** | 0.763 | 0.582 | 0.001** |
| (EVI) | 0.743 | 0.553 | 0.005** | 0.749 | 0.561 | 0.008** |
| (GNDVI) | 0.823 | 0.675 | 0.329 | 0.876 | 0.767 | 0.2087 |
| (LAI) | 0.897 | 0.805 | 0.002** | 0.820 | 0.673 | 0.000** * |

Source: WorldView2 data, July 2018 [18].

Using Worldview 2 image as a high spatial resolution satellite imagery for corn plants Calcium and Potassium content detection

Table 4 demonstrates the regression analysis and the fitting models of the relationship between corn plants dry matter Ca and K

content and the published vegetation indices extracted from the WV 2 image. The majority of vegetation indices had negative relationships with the concentration of both elements. With R^2 values of 0.9013, 0.8019, 0.8997, and 0.783 respectively, DVI, EVI, and GNDVI performed well in estimating plant dry matter Ca and K content with high significant level P -value < 0.001 . LAI had a significant effect with P -value < 0.5 for both two elements. Figure 3 depict the relationships between Ca and K concentration in corn dry matter and the most highly correlated vegetation indices.

Table 4. Fitting model, R^2 , and P -value for the relationship between WorldView 2 VIs and calcium and potassium accumulation into the corn dry matter

| VIs | WorldView 2 Image | | |
|--|--|--------|---------------|
| | Corn plants dry matter Calcium content | | |
| | Fitting model | R^2 | P - Value |
| DVI | $Y = -0.8763X + 2.4727$ | 0.9013 | < 0.001 *** |
| EVI | $Y = -0.7661X + 2.626$ | 0.8019 | < 0.001 *** |
| GNDVI | $Y = -1.9743X + 3.7517$ | 0.8997 | < 0.001 *** |
| LAI | $Y = -0.2144X + 2.6046$ | 0.783 | 0.406 * |
| Corn plants dry matter potassium content | | | |
| DVI | $Y = -0.701X + 1.9782$ | 0.9013 | < 0.001 *** |
| EVI | $Y = -0.6129X + 2.1008$ | 0.8019 | < 0.001 *** |
| GNDVI | $Y = -1.5794X + 3.0013$ | 0.8997 | < 0.001 *** |
| LAI | $Y = -0.1715X + 2.0837$ | 0.783 | 0.1138* |

Source: calculations from worldview2 satellite image , July 2018 [18].

Using Sentinel 2 image as a moderate spatial resolution satellite imagery for corn plants Calcium content detection

The regression analysis and fitting models of the relationship between corn plants dry matter Ca content and reported vegetation indices extracted from the Sentinel 2 image are shown in Table 5. The concentrations of the element had negative relationship with the majority of vegetation indices. DVI, EVI, GNDVI, and LAI performed well in estimating plant dry matter Ca content with R^2 values of 0.566, 0.5647, 0.3306, and 0.5647, respectively, with a high significant level P -value 0.001.

LAI had a statistically significant impact with a P -value of 0.5. The relationships between the concentrations of calcium and potassium in corn dry matter and the most closely associated vegetation indices are depicted in Fig. 4.

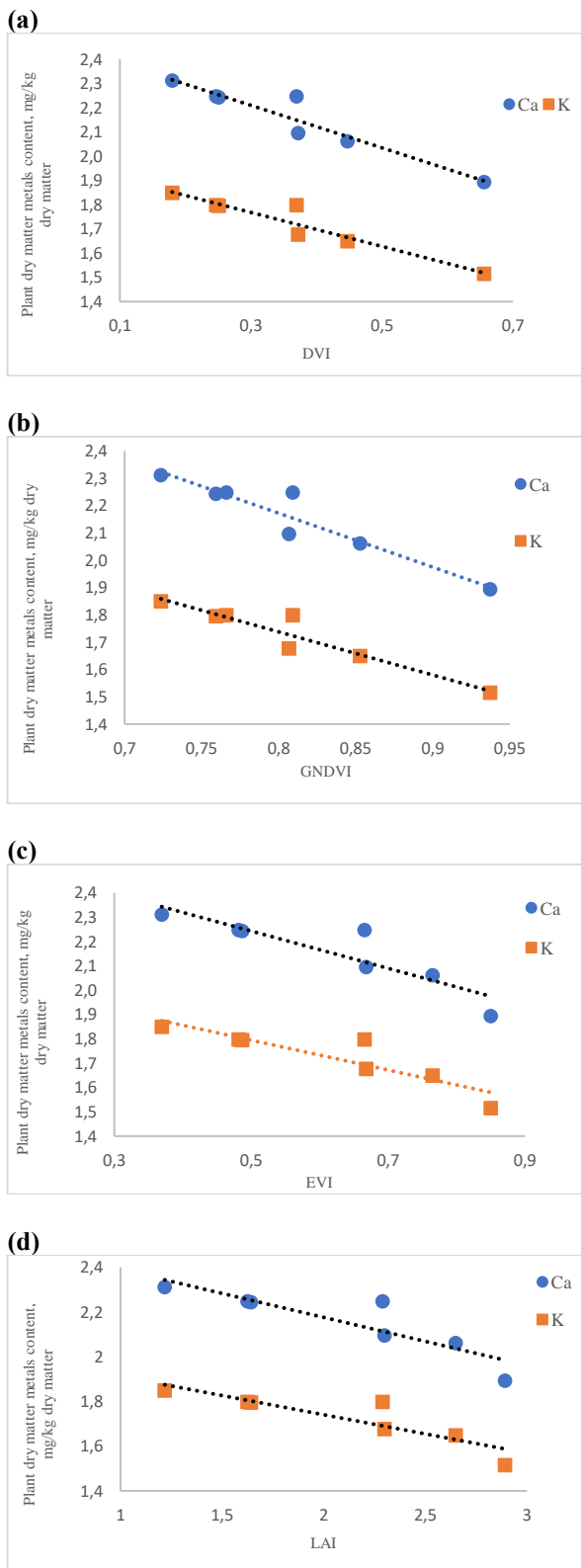


Fig. 3. Relationship between above ground plant dry matter Ca and K content and vegetation indices calculated from WorldView 2 satellite image
 Source: calculations from worldview2 satellite image , July 2018 [18].

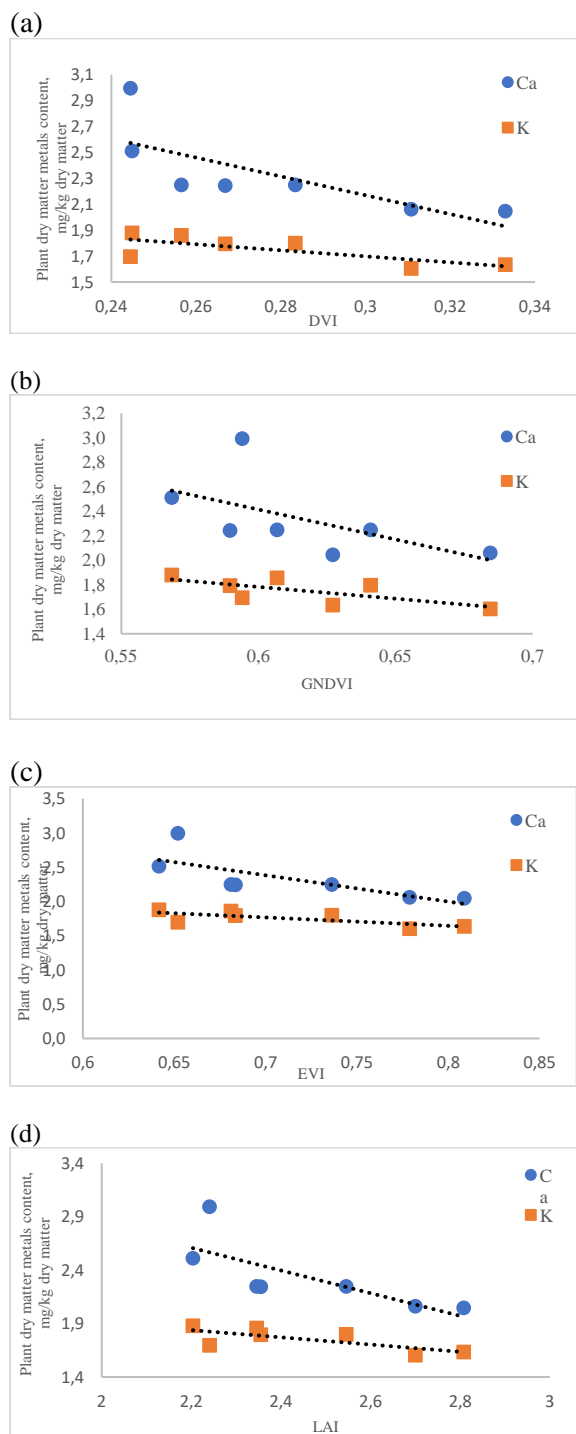


Fig. 4. Relationship between above ground plant dry matter Ca and K content and vegetation indices calculated from Sentinel 2 satellite image
 Source: calculations from Sentinel 2 satellite image, July 2018 [12].

Using Sentinel 2 image as a moderate spatial resolution satellite imagery for corn plants Potassium content detection

Table 5 shows the regression analysis and fitting models for the relationship between dry matter K content of corn plants and recorded vegetation indices extracted from the Sentinel

2 image. The majority of vegetation indices showed a negative correlation with the element's concentrations. With R^2 values of 0.5343, 0.524, 0.4694, and 0.524 respectively, DVI, EVI, GNDVI, and LAI performed well in estimating plant dry matter K material with a P-value < 0.01, LAI was statistically important. The associations between calcium and potassium concentrations in corn dry matter and the most closely related vegetation indices are shown in Fig. 4.

Table 5. Fitting model, R^2 , and P-value for the relationship between Sentinel 2 VIs and calcium and potassium accumulation into the corn dry matter

| VIs | Sentinel 2 Image | | |
|--|--|--------|------------|
| | Corn plants dry matter Calcium content | | |
| | Fitting model | R^2 | P - Value |
| DVI | $Y = -7.2697X + 4.3503$ | 0.566 | < 0.001*** |
| EVI | $Y = -3.8419X + 5.07$ | 0.5647 | < 0.001*** |
| GNDVI | $Y = -4.8848X + 5.3443$ | 0.3306 | < 0.001*** |
| LAI | $Y = -1.0619X + 4.9447$ | 0.5647 | 0.28* |
| Corn plants dry matter potassium content | | | |
| DVI | $Y = -2.3317X + 2.3977$ | 0.5343 | < 0.001*** |
| EVI | $Y = -1.2217X + 2.621$ | 0.524 | < 0.001*** |
| GNDVI | $Y = -1.9214X + 2.935$ | 0.4694 | < 0.001*** |
| LAI | $Y = -0.3377X + 2.5812$ | 0.524 | 0.001** |

Source: calculations from worldview2 satellite image, July 2018 [18].

CONCLUSIONS

This study compared the using of multi-temporal Sentinel-2 images with the high resolution Worldview 2 image to detect Ca and K concentration on corn plants growing in a natural agriculture ecosystem irrigated with industrial waste water on the regional scale. (DVI), (EVI), (GNDVI), and (LAI) were selected as an effective indicator for Ca and K corn plants content based on data measured in the field and comparisons between ASD VIs, Sentinel-2 VIs, and WorldView 2 VIs, and these results also proved that the Sentinel-2 images are an effective remote data source for detecting plant stress.

The price volatility is reflected at all chin stages level and especially at the production stage and to a lesser degree at the marketing and processing levels.

REFERENCES

[1]Boegh, E., Soegaard, H., Broge, N., Hasager, C., Jensen, N., Schelde, K., Thomsen, A., 2002. Airborne

multispectral data for quantifying leaf area index, nitrogen concentration, and photosynthetic efficiency in agriculture. *Remote sensing of environment*, 81(2-3), 179-193.

[2] Bruzzone, L., Bovolo, F., 2012, A novel framework for the design of change-detection systems for very-high-resolution remote sensing images. *Proceedings of the IEEE*, 101(3), 609-630.

[3] Download QGIS, QGIS 2.18.3 software, <https://qgis.org/en/site/forusers/download.html>, Accessed on July 2018

[4] European space agency, 2018, <http://www.esa.int/>, Accessed on June 2018

[5] Gholizadeh, A., Kopačková, V., 2019, Detecting vegetation stress as a soil contamination proxy: a review of optical proximal and remote sensing techniques. *International Journal of Environmental Science and Technology*, 16(5), 2511-2524. doi:10.1007/s13762-019-02310-w, Accessed on May 2021

[6] Gitelson, A. A., Merzlyak, M. N., 1998, Remote sensing of chlorophyll concentration in higher plant leaves. *Advances in Space Research*, 22(5), 689-692.

[7] Huete, A., Didan, K., Miura, T., Rodriguez, E. P., Gao, X., Ferreira, L. G., 2002, Overview of the radiometric and biophysical performance of the MODIS vegetation indices. *Remote sensing of environment*, 83(1-2), 195-213.

[8] Mahmoudzadeh, H., 2007, Digital change detection using remotely sensed data for monitoring green space destruction in Tabriz.

[9] Naveena D., R., Jiji, G. W., 2015, Change Detection Techniques - A Survey. *International Journal on Computational Science & Applications*, 5(2), pp.45-57.

[10] Nelson, R. F., 1983, Detecting forest canopy change due to insect activity using Landsat MSS. *Photogrammetric Engineering and Remote Sensing*, 49(9), 1303-1314.

[11] Panuju, D. R., Paull, D. J., Griffin, A. L., 2020, Change Detection Techniques Based on Multispectral Images for Investigating Land Cover Dynamics. *Remote Sensing*, 12(11). doi:10.3390/rs12111781, Accessed on May 2021

[12] Sentinel 2 Imagery, <https://eos.com/find-satellite/sentinel-2/>, Accessed on July 2018

[13] Sentinel hub, 2018, <https://www.sentinel-hub.com/>, Accessed on July 2018

[14] Shi, T., Wang, J., Chen, Y., Wu, G., 2016, Improving the prediction of arsenic contents in agricultural soils by combining the reflectance spectroscopy of soils and rice plants. *International Journal of Applied Earth Observation and Geoinformation*, 52, 95-103. doi:10.1016/j.jag.2016.06.002, Accessed on April 2018

[15] Tucker, C. J., 1979, Red and photographic infrared linear combinations for monitoring vegetation. *Remote sensing of environment*, 8(2), 127-150.

[16] Tüshaus, J., Dubovik, O., Khamzina, A., Menz, G., 2014, Comparison of medium spatial resolution ENVISAT-MERIS and terra-MODIS time series for

vegetation decline analysis: A case study in central Asia. *Remote Sensing*, 6(6), pp.5238-5256.

[17] Vegetation Indices Harris Geospatial solutions, <https://www.l3harrisgeospatial.com/docs/vegetationindices.html>, Accessed on July 2018

[18] WorldView 2 Satellite Sensor, <https://www.satimagingcorp.com/satellite-sensors/worldview-2/>, June 2018

[19] Zarco-Tejada, P. J., González-Dugo, V., Berni, J. A., 2012, Fluorescence, temperature and narrow-band indices acquired from a UAV platform for water stress detection using a micro-hyperspectral imager and a thermal camera. *Remote sensing of environment*, 117, 322-337.

[20] Zheng, H., Cheng, T., Li, D., Zhou, X., Yao, X., Tian, Y., Cao, W., Zhu, Y., 2018, Evaluation of RGB, color-infrared and multispectral images acquired from unmanned aerial systems for the estimation of nitrogen accumulation in rice. *Remote Sensing*, 10(6), 824.